

MRI investigation of functional connectivity in the human spinal cord

Oscar San Emeterio Nateras¹, Fang Yu², Eric R Muir^{3,4}, Carlos Bazan III², Crystal G Franklin⁴, Wei Li^{3,4}, Jack L Lancaster^{2,4}, Jinqi Li^{2,4}, and Timothy Q Duong^{3,4}
¹Biomedical Engineering, University of Texas at San Antonio, San Antonio, Texas, United States, ²Radiology, University of Health Science Center at San Antonio, Texas, United States, ³Ophthalmology, University of Health Science Center at San Antonio, Texas, United States, ⁴Research Imaging Institute, San Antonio, Texas, United States

Target Audience spinal cord and resting-state functional MRI (rsfMRI)

Purpose To apply resting-state functional MRI (rsfMRI) to map functional connectivity networks of the human spinal cord. The technical challenges and solutions to obtain robust rsfMRI data are detailed. Intra- and inter-subject reproducibility was also quantitatively evaluated. Moreover, 3D rsfMRI maps facilitated visualization of the functional connectivity along the length of the spinal cord. Results were interpreted with respect to known anatomical and functional structures of the spinal cord.

Methods Ten self-declared normal volunteers were studied. Independent-component analysis (ICA) was employed obtained rsfMRI maps. Reproducibility was assessed on a single subject, where 4 repeated BOLD rsfMRI scans were acquired in a single session. For each subject, 4 repeated BOLD rsfMRIs were performed at 3T using a neck RF coil, covering the bottom of C1 to C4. rsfMRI was obtained using gradient-echo (EPI), with a FOV=128x128mm, matrix=128x128 (1x1x3mm resolution), TR=2s, TE=26ms, Thk=3mm, 23 axial slices, and 300 time points (10 min). T2-weighted anatomical images were obtained using a TSE sequence with a FOV=128x128 mm, matrix=128x128 (1x1x3mm resolution), TR=6.9s, TE=70 ms, flip angle 150°, NT=2, and ETL=9. QSM image was acquired using TR=61ms, TE=4.51ms, number of echoes=12 with TE ranging from 4.51 to 49.59 ms, FOV=128x128mm, and matrix=320x320 (0.4x0.4x3mm resolution).

Data Analysis: Motion corrected BOLD images were co-registered to each subject's own T2-weighted anatomical image using the transform tool in MANGO v3.11. The co-registration was done manually using one spinal cord ROI (from the reference subject) as a guide to align the images via rotation, translation, and scaling of the images. Individual data sets were then co-registered to a reference template (obtained from one of the subject) for group analysis. Individual subject data were de-noised using ICA method. With the spinal cord ROI the cerebrospinal fluid (CSF) pixels were excluded. A high-pass filter of 100 s cutoff and a 2mm spatial filter were applied. The number of independent components (ICs) set to 16. ICs were overlaid on the reference subject's QSM images. A neck brace was used to reduce motion artifacts and facilitated co-registration.

Results Anatomical MRI of the spine from C1-C4 provided excellent grey-white matter contrast in the spinal cord. ICA de-noising analysis isolated a few strong coherences in the surrounding cerebral spinal fluid (CSF), likely the result of pulsatile CSF artifacts (**Figure 1a**). Thus, subsequent rsfMRI analysis included the use of ICA de-noising and an anatomically defined spinal cord mask (**Figure 1b**). Quantitative analysis of the ICA components showed reproducibility (**Figure 2**): The mean z-score was the same for the three components analyzed ($z = 6 \pm 1$). The centroid coordinates were very similar across trials, deviating by 2 for in-plane voxels and up to 1 adjacent image slice. **Figure 3** shows 16 ICs rsfMRI connectivity maps of the group data, ordered anatomically from superior to inferior position. The rsfMRI components showed robust network of connectivity in the spinal cord, with coherence patterns predominantly localized to GM. Bilateral, unilateral, and intersegmental coherence patterns were detected. Some ICs had bilateral and intersegmental activation patterns (#1, 2, 5, and 13), while others showed unilateral and intersegmental activation (#4, 10, and 15). Only IC# 6, 8, and 11 showed definite unilateral activation, while IC# 3, 7, 9, 12, 14, and 16 showed mainly centralized activation but also had some lateral activation.

Discussion and Conclusions Previous study investigated rsfMRI of the spinal cord at 1.5 T on single subjects with limited successes.¹ On group data, Barry et al. used seed-based rsfMRI analysis to investigate C3 to C5 with a 0.91x0.91x4mm resolution at 7T.² They found correlations between left and right ventral as well as dorsal horns, consistent with our study. No significant correlation between GM and WM were observed, suggesting the rsfMRI activation localized in the GM were unlikely due to spatial correlated physiological noise. Data were also presented on individual 2D slices in contrast with ICA that also correlates the data along the length of the spinal cord. We found it helpful to first mask spinal cord before co-registration and rsfMRI ICA analysis. A similar approach has been applied to mask rsfMRI of the brainstem.⁵ Detailed interpretations of the intrinsic connectivity network will likely benefit from improved spatial resolution. Nonetheless, this study demonstrates a novel rsfMRI application to investigate the spinal cord. We detected an elaborate functional network in the spinal C1-C4, and they included unilateral, bilateral and rostro-caudal functional connectivity. Future studies will improve spatial resolution to distinguish different functional structures, validate the functional networks, and to map connectivity of the entire spinal cord to the brain. This approach set the stage for exploring clinical applications (such as post-traumatic injuries and neurodegenerative conditions).

REFERENCES (1) Wei et al. Eur J Appl Physiol 2010;108:265. (2) Barry et al. eLife. 2014;3:e02812. (3) Yoshizawa et al. Neuroimage 1996;4:174. (4) Cadotte et al. J Neurosurg Spine 2012;17:102. (5) Beissner et al. NeuroImage. 2014;86:91-8.

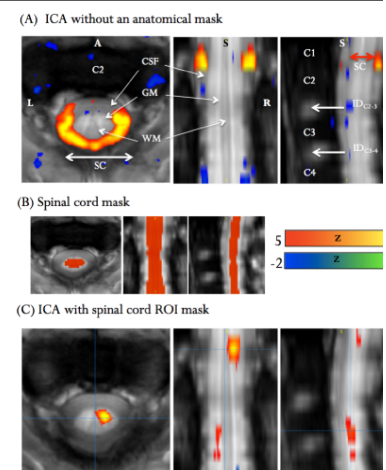


Figure 1. Independent component analysis (ICA) of rsfMRI spinal cord maps from one subject.

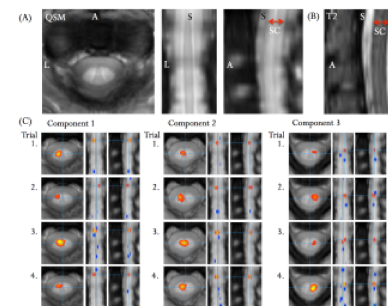


Figure 2. Anatomical images (A) Susceptibility, (B) T2-weighted, (C) Reproducibility of rsfMRI connectivity maps.

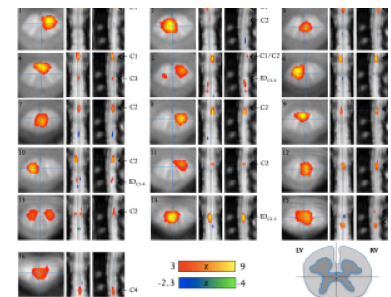


Figure 3. Group resting-state fMRI data showing 16 ICA components (N=10).

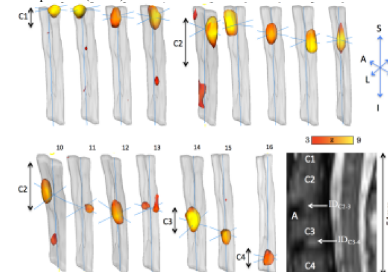


Figure 4. 3D surface rendering of 16 connectivity maps showing the location and extent of each ICA components.